J Solution Chem (2015) 44:703–717
DOI 10.1007/s10953-015-0326-0

Thermophysical Properties of Two Ammonium-Based Protic Ionic Liquids

Arijit Bhattacharjee[1] · João A. P. Coutinho[1] · Mara G. Freire[1] · Pedro J. Carvalho[1]

Received: 25 September 2014 / Accepted: 20 November 2014 / Published online: 5 April 2015

Abstract Experimental data for density, viscosity, refractive index and surface tension are reported, for the first time, in the temperature range between 288.15 and 353.15 K and at atmospheric pressure for two protic ionic liquids, namely 2-(dimethylamino)-*N*,*N*-dimethylethan-1-ammonium acetate, $[N_{11\{2(N11)\}H}][CH_3CO_2]$, and *N*-ethyl-*N*,*N*-dimethylammonium phenylacetate, $[N_{112H}][C_7H_7CO_2]$. The effect of the anion's aromaticity and the cation's aliphatic tails on the studied properties is discussed. Additional derived properties, such as isobaric thermal expansion coefficient, surface entropy and enthalpy and critical temperature, were estimated.

Keywords Protic ionic liquids · Density · Viscosity · Refractive index · Surface tension

1 Introduction

Ionic liquids (ILs) are an exciting class of solvents, receiving enormous attention in recent years as potential replacements for conventional organic solvents in a wide range of applications. They are defined as salts with a melting point lower than 373 K [1] and have emerged as unique and versatile solvents and materials with unique properties. In contrast to conventional organic solvents, ILs usually have extremely low volatility, good thermal and chemical stabilities, a large liquid temperature range and a very good solvation ability for a wide variety of compounds [1]. ILs have been seen as "designer solvents" or "task-specific fluids" due to the fact that different combinations of their ions and the introduction of specific and functionalized groups lead to significant changes in their thermophysical properties and phase behavior, adapting them to use in specific applications. This feature

✉ Pedro J. Carvalho
quijorge@ua.pt

[1] CICECO - Aveiro Institute of Materials, Department of Chemistry, University of Aveiro, 3810-193 Aveiro, Portugal

created a tremendous potential of ILs as alternatives for conventional solvents in catalysis [2, 3], electrochemistry [4, 5], organic reactions [6], biocatalysis and enzymes [7, 8], fuel cells [9], batteries [10], sensors [11] and solar cells [12].

ILs can be divided into two main families, viz. aprotic ionic liquids (AILs) and protic ionic liquids (PILs). AILs can be synthesized by transferring any group other than a proton to a basic site on the basic parent molecule. PILs are complex liquids, formed by proton transfer from a Brønsted acid to a Brønsted base and their main difference, compared to AILs, is the presence of at least one proton which is/are able to participate in extensive hydrogen bonding [13]. Greaves et al. [14] discussed the known range of PILs, including their reported physicochemical properties and the applications where they have been used. To date, AILs have received more attention than PILs but, recently, there has been an increasing interest in PILs due to their highly mobile proton and its impact on the common tailored properties. The emphasis on PILs lies in their low cost, simplicity of synthesis and variety of applications of this new family of ILs [14–18]. Moreover, this kind of ILs seem to have low toxicities [19]. Their protic nature is determinant in a number of uses including biological applications [20], organic synthesis [21–23], chromatography [24], as electrolytes for polymer membrane fuel cells [25], as reactants in biodiesel production [26], and as propellant or explosives [27, 28]. Consequently, available physicochemical properties or thermodynamic databases of PILs can be of technological and/or theoretical interest. Experimental studies of thermophysical properties of ILs have been largely reported for imidazolium-, pyridinium-, piperidinium-, pyrrolidinium-, sulfonium- and for some ammonium-based ILs, which are based in primary ammine cations of the form R_4N^+. Recently, the general properties of ammonium-based PILs have been the subject of some structure–property relationship studies [14, 17, 29–41].

The objective of this work is to investigate and thus provide an insight into the cation and anion effects through the measured and derived thermophysical properties of PILs, and to study the relationship between the measured properties and their ionic structures aiming at establishing fundamental principles for the molecular design of ILs. In this work, density, viscosity, refractive index and surface tension data of two PILs, namely 2-(dimethylamino)-*N*,*N*-dimethylethan-1-ammonium acetate, $[N_{11\{2(N11)\}H}][CH_3CO_2]$, and *N*-ethyl-*N*,*N*-dimethylammonium phenylacetate, $[N_{112H}][C_7H_7CO_2]$, were measured as a function of temperature in the temperature range between 283.15 and 353.15 K and at atmospheric pressure. Additional properties, such as the isobaric thermal expansion coefficient, the surface thermodynamic properties, and critical temperature of both PILs were also estimated.

2 Materials and Methods

2.1 Materials

Two PILs were studied in this work, namely 2-(dimethylamino)-*N*,*N*-dimethylethan-1-ammonium acetate, $[N_{11\{2(N11)\}H}][CH_3CO_2]$ (CAS Registry No. CS-0463-HP-0100), and *N*-ethyl-*N*,*N*-dimethylammonium phenylacetate, $[N_{112H}][C_7H_7CO_2]$ (CAS Registry No. CS-0466-HP-0100). These PILs were acquired from IoLiTec with mass fraction purities higher than 98 %. The ionic structures and description of the studied PILs are presented in Table 1.

Table 1 Ionic structure, compound description, molecular weight, and water content of the studied ILs

IL	Ionic structure
2-(dimethylamino)-*N,N*-dimethylethan-1-ammonium acetate $[N_{11\{2(N11)\}H}][CH_3CO_2]$ (176.3 g·mol^{-1}; water wt% = 0.0678 %)	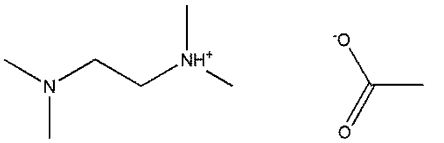
N-ethyl-*N,N*-dimethylammonium phenylacetate $[N_{112H}][C_7H_7CO_2]$ (207.3 g·mol^{-1}; water wt% = 0.0278 %)	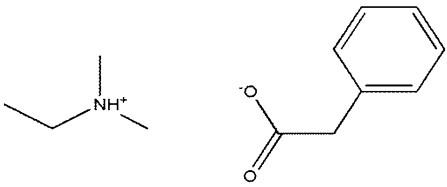

The $[N_{11\{2(N11)\}H}][CH_3CO_2]$ was distilled at room temperature, under constant stirring and high vacuum ($\approx 10^{-1}$ Pa). The initial fraction of about 5 mL was discarded in order to remove water and solvents derived from the synthesis of the IL. The remaining IL was further distilled and the distillate used. Before each measurement the IL was further distilled (discarding small initial fractions) to remove traces of water adsorbed during the IL manipulation. The $[N_{112H}][C_7H_7CO_2]$ was dried at moderate temperature ($\approx$313 K), under vacuum ($\approx 10^{-1}$ Pa) and under continuous stirring, for a minimum period of 48 h in order to remove traces of water and volatile compounds.

The purity of each IL was checked by ^{1}H and ^{13}C NMR, both before and after the measurements, to assure that no degradation occurred. The final IL water content, after the drying step and immediately before the measurements, was determined with a Metrohm 831 Karl Fischer coulometer (using the Hydranal - Coulomat AG from Riedel-de Haën as analyte). The average water content, the molecular weight and the mass purity of each PIL are presented in Table 1.

2.2 Experimental Section

2.2.1 Density and Viscosity

Density (ρ) and dynamic viscosity (η) measurements were carried out using an automated SVM3000 Anton Paar rotational Stabinger viscometer–densimeter in the temperature range from 283.15 to 353.15 K and at atmospheric pressure ($\approx$0.1 MPa). The absolute uncertainty in density is $\pm 5 \times 10^{-4}$ g·cm^{-3}, and the relative uncertainty in dynamic viscosity is $\pm$1 %. The relative uncertainty in temperature is within $\pm$0.02 K. Further details regarding the use of the equipment and methodologies for the determination of densities and viscosities can be found elsewhere [42, 43].

2.2.2 Refractive Index

Measurements of refractive index (n_D) were performed at 589.3 nm using an automated Abbemat 500 Anton Paar refractometer. Refractive index measurements were carried out in the temperature range from 283.15 to 353.15 K and at atmospheric pressure. The Abbemat 500 Anton Paar refractometer uses reflected light to measure the refractive index,

where the sample on the top of the measuring prism is irradiated from different angles by a light-emitting diode (LED). The maximum deviation in temperature is ±0.05 K, and the maximum uncertainty in the refractive index measurements is $\pm 2 \times 10^{-4}$ n_D. The capability of the equipment to determine accurate refractive indices of ILs has been previously verified [36, 44–46].

2.2.3 Surface Tension

The surface tension of each IL was determined through the analysis of the shape of a pendant drop using a Data Physics OCA-20 (Data Physics Instruments GmbH, Germany). Pendant drops were created using a Hamilton DS 500/GT syringe connected to a Teflon coated needle placed inside an aluminium air chamber capable of maintaining the temperature within ±0.1 K. The temperature was maintined by circulating water in the double jacketed aluminium cell by means of a Julabo F-25 water bath. The temperature inside the aluminium chamber was measured with a Pt100 platinum thermometer which was at a distance of approximately 2 cm from the drop. The surface tension measurements were performed in the temperature range from 293 to 344 K and at atmospheric pressure. After reaching a specific temperature, the drop was formed and the measurements were carried out after 30 min to guarantee the thermal equilibrium. Silica gel was kept inside the air chamber to maintain a dry atmosphere. For the surface tension determination, at each temperature and for each IL, at least three drops were formed and analyzed. For each drop an average of 100 images were captured. The analysis of the drop shape was achieved with

Table 2 Densities (ρ), molar volumes (V_m), viscosities (η) and refractive index values (n_D) of the studied PILs as a function of temperature and at atmospheric pressure

T/K	$[N_{11\{2(N11)\}H}][CH_3CO_2]$				$[N_{112H}][C_7H_7CO_2]$			
	ρ/kg·m^{-3}	$10^6 V_m$/ m^3·mol^{-1}	η/mPa·s	n_D	ρ/kg·m^{-3}	$10^6 V_m$/ m^3·mol^{-1}	η/ mPa·s	n_D
283.15	1017.9	173.2	64.8	1.44000	1109.9	188.6	413.1	1.53585
288.15	1013.5	173.9	46.3	1.43807	1106.1	189.2	269.6	1.53415
293.15	1009.1	174.7	34.0	1.43612	1102.5	189.8	185.3	1.53239
298.15	1004.7	175.4	25.9	1.43401	1098.9	190.4	130.8	1.53064
303.15	1000.4	176.2	20.2	1.43222	1095.4	191.1	96.00	1.52889
308.15	996.3	176.9	16.0	1.43024	1091.8	191.7	72.45	1.52707
313.15	991.9	177.7	12.9	1.42834	1088.3	192.3	56.16	1.52530
318.15	987.6	178.5	10.7	1.42642	1084.8	192.9	44.27	1.52340
323.15	983.3	179.3	8.92	1.42443	1081.3	193.5	35.62	1.52153
328.15	978.9	180.1	7.54	1.42250	1077.8	194.2	29.13	1.51965
333.15	974.6	180.9	6.44	1.42055	1074.3	194.8	24.22	1.51774
338.15	970.2	181.7	5.58	1.41861	1070.8	195.4	20.30	1.51590
343.15	965.9	182.5	4.86	1.39616	1067.3	196.1	17.25	1.51410
348.15	961.6	183.3	4.28	1.39486	1063.8	196.7	14.80	1.51216
353.15	957.2	184.1	3.78	1.39358	1060.4	195.5	12.85	1.51032

Standard temperature uncertainty is $u(T) = \pm 0.02$ K and the combined expanded uncertainties, U are $U(\rho) = \pm 0.5$ kg·m^{-3}; $U(\eta) = 0.1$ %; $U(n_D) = 2 \times 10^{-4}$ with 95 % confidence level

the software module SCA 20. The IL density data required to the surface tension determination were those determined in this work. The equipment was previously validated through the measurement of the surface tension of ultra-pure water, *n*-decane and *n*-dodecane, as well as for a large number of ILs and IL families [45–47].

3 Results and Discussion

3.1 Density

The experimental densities of the two PILs are reported in Table 2 and shown in Fig. 1. To the best of our knowledge no literature data are available. As commonly observed, the alkyl chains size and an increase on the IL asymmetry lead to weaker intermolecular interactions and more bulk entanglement and thus to lower densities displayed by $[N_{11\{2(N11)\}H}][CH_3CO_2]$ [36, 46, 48–51]. Furthermore, the presence of an aromatic ring is known to lead to higher intermolecular interactions, and thus to the higher densities of $[N_{112H}][C_7H_7CO_2]$ compared to $[N_{112H}][CH_3CO_2]$, previously measured [36], or the $[N_{11\{2(N11)\}H}][CH_3CO_2]$. Nevertheless, it should be remarked that the lack of data for other anions precludes more conclusive analysis.

Molar volumes (V_m) were calculated as function of temperature and up to 353.15 K and are reported in Table 2. As commonly observed, the molar volumes increase with the temperature increase and follow the opposite trend of the densities, with $[N_{11\{2(N11)\}H}][CH_3CO_2]$ presenting lower molar volumes than $[N_{112H}][C_7H_7CO_2]$ due to the larger volume of phenylacetate (1133.79 nm^3) when compared with acetate (488.49 nm^3), as obtained from COSMO-RS [52, 53].

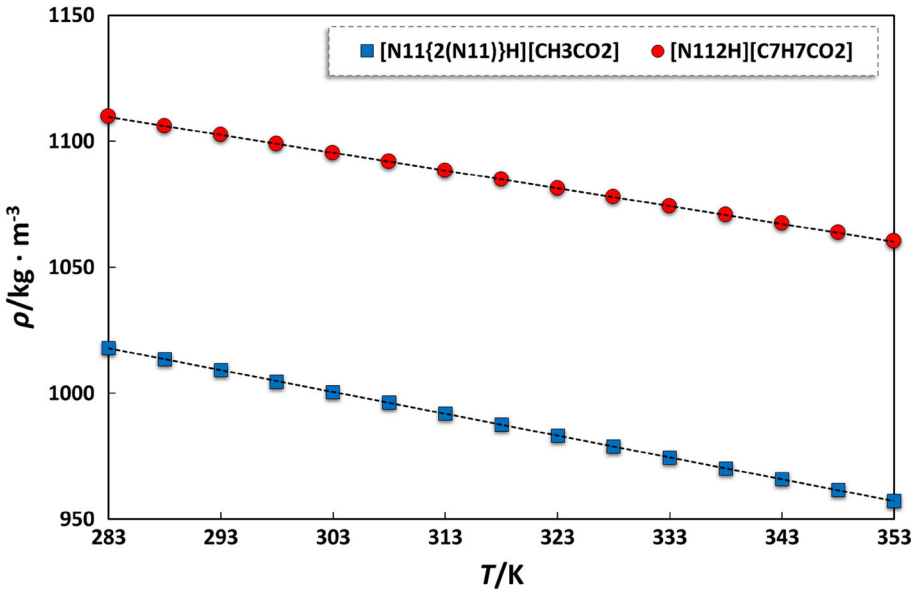

Fig. 1 Density as function of temperature for the studied PILs. The *dotted lines* represent the linear fit to the experimental data

The isobaric thermal expansion coefficients (α_p), which consider the volumetric changes with temperature, were estimated from the linear density dependency with temperature using the following equation:

$$\alpha_p = -\frac{1}{\rho}\left(\frac{\partial \rho}{\partial T}\right)_p = -\left(\frac{\partial \ln \rho}{\partial T}\right)_p \quad (1)$$

where ρ is the density in kg·m^{-3}, T the temperature in K, and p the pressure in MPa.

In Table 3, α_p is presented for the PILs. The values of α_p for $[N_{112H}][C_7H_7CO_2]$ $(6.499 \pm 0.001) \times 10^{-4}$ K^{-1} and $[N_{112H}][CH_3CO_2]$ $(7.7 \times 10^{-4}$ K$^{-1})$ [36] are lower than that of $[N_{11\{2(N11)\}H}][CH_3CO_2]$ $(8.762 \pm 0.001) \times 10^{-4}$ K^{-1}, denoting the lower thermal expansion of the smaller alkyl chain ILs, compared to those with longer chains, as is commonly observed. Furthermore, if one compares the thermal expansion coefficient of $[N_{112H}][C_7H_7CO_2]$ and $[N_{112H}][CH_3CO_2]$ [36], it is seen that the phenylacetate IL presents lower thermal expansion.

3.2 Viscosity

The viscosity is an important macroscopic property of ILs, which is the consequence of several microscopic interactions such as columbic, van der Waals and hydrogen bonding, and is quite dependent upon the shape and size of the constituent ions. It affects ionic conductivity and mass transport phenomena, thereby restricting their suitability for particular applications. The experimental viscosities of the PILs from 283.15 to 353.15 K are shown in Fig. 2 and summarized in Table 2. As is commonly reported in the literature and as discussed in the density section, the size of the alkyl chains and the IL asymmetry leads to more entanglement [36, 45, 46, 48–51], that in turn leads to a higher resistance to shear stress and therefore to higher viscosities as displayed by $[N_{11\{2(N11)\}H}][CH_3CO_2]$ and $[N_{112H}][CH_3CO_2]$ [36]. Furthermore, the presence of an aromatic ring, known to lead to higher intermolecular interactions, also contributes to the higher viscosities displayed by the $[N_{112H}][C_7H_7CO_2]$ when compared to $[N_{11\{2(N11)\}H}][CH_3CO_2]$ and $[N_{112H}][CH_3CO_2]$

Table 3 Coefficients of thermal expansion (α_p), refractive indices (n_D), isotropic polarizabilities, derived molar refractions (R_m) and free volumes (f_m), at 298.15 K; surface entropy (S^{γ}), surface enthalpy (H^{γ}) and estimated critical temperatures using both Eötvös $(T_c)_{Eot}$ [68] and Guggenheim $(T_c)_{Gug}$ [69] empirical equations for the studied ILs

	$[N_{11\{2(N11)\}H}][CH_3CO_2]$	$[N_{112H}][C_7H_7CO_2]$
$10^4 \cdot (\alpha_p \pm \sigma)^a$/K^{-1}	8.762 ± 0.001	6.499 ± 0.001
n_D	1.43401	1.53064
Polarizability/bohr^3	122.22	157.54
R_m/cm^3·mol^{-1}	45.69	58.89
f_m/cm^3·mol^{-1}	129.75	131.56
$10^5 \cdot (S^{\gamma} \pm \sigma)^a$/J·m^{-2}·K^{-1}	10.7 ± 0.33	11.0 ± 0.24
$10^2 \cdot (H^{\gamma} \pm \sigma)^a$/J·m^{-2}	6.52 ± 0.10	7.61 ± 0.08
$(T_c)_{Eot}$/K	673 ± 12	773 ± 11
$(T_c)_{Gug}$/K	669 ± 14	762 ± 13

[a] Expanded uncertainty with an approximately 95 % level of confidence

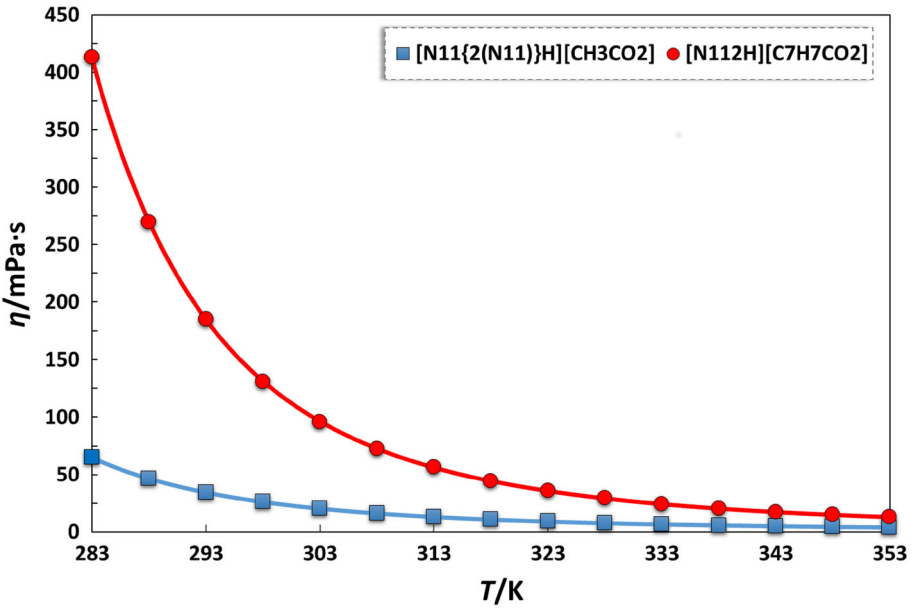

Fig. 2 Viscosity data for the studied ILs. The *solid lines* represent the Vogel–Fulcher–Tammann (VFT) group contribution correlation [54]

[36]. The $[N_{112H}][C_7H_7CO_2]$ viscosity is one order of magnitude higher than that obtained for $[N_{112H}][CH_3CO_2]$ previously measured by us [36].

The description of viscosities for the pure PILs was fitted using the group contribution method, based on the Vogel–Fulcher–Tammann (VFT) correlation [54], represented by the following equation:

$$\ln \eta = A_\eta + \frac{B_\eta}{(T - T_{0\eta})} \tag{2}$$

where η is the dynamic viscosity in mPa·s, T the temperature in K, and A_η, B_η and $T_{0\eta}$ are adjustable parameters.

The parameters A_η, B_η and $T_{0\eta}$ were determined from fitting of the experimental data and are presented in Table 4. The fitting of the data against the experimental results is depicted in Fig. 2 and presents average absolute relative deviations, between the experimental and the fitting data, of 0.15 % for $[N_{11\{2(N11)\}H}][CH_3CO_2]$ and 0.18 % for $[N_{112H}][C_7H_7CO_2]$.

Table 4 Vogel–Fulcher–Tammann correlation parameters, A_η, B_η and $T_{0\eta}$, for the viscosity of the studied ILs

IL	A_η	B_η/K	$T_{0\eta}$/K
$[N_{11\{2(N11)\}H}][CH_3CO_2]$	−2.4822	626.40	188.99
$[N_{112H}][C_7H_7CO_2]$	−1.7662	679.41	195.88

3.3 Refractive Index

Experimental refractive indexes for the studied compounds are presented in Table 2 and shown in Fig. 3. The temperature interval was scanned upward and downward and no temperature hysteresis effects were observed. For the two PILs under study, the refractive index decreases with an increase in temperature. Furthermore, the refractive index values for the studied PILs increase in the following sequence: $[N_{112H}][CH_3CO_2]$ [36] < $[N_{11\{2(N11)\}H}][CH_3CO_2]$ < $[N_{112H}][C_7H_7CO_2]$.

The refractive indices for the PILs studied were also fitted to the group contribution method proposed by Gardas and Coutinho [54], as depicted in Fig. 3, which follows a linear temperature dependency of the form,

$$n_D = A_{n_D} - B_{n_D} T \tag{3}$$

$$A_{n_D} = \sum_{i=1}^{k} n_i a_{i,n_D} \tag{4}$$

$$B_{n_D} = \sum_{i=1}^{k} n_i b_{i,n_D} \tag{5}$$

where n_i is the number of groups of type i and k is the total number of different groups in the molecule. The estimated parameters a_{i,n_D} and b_{i,n_D} for the studied ILs are given in Table 5. The average absolute relative deviation between the experimental and the fitting values are 0.0043 % for $[N_{11\{2(N11)\}H}][CH_3CO_2]$ and 0.0062 % for $[N_{112H}][C_7H_7CO_2]$.

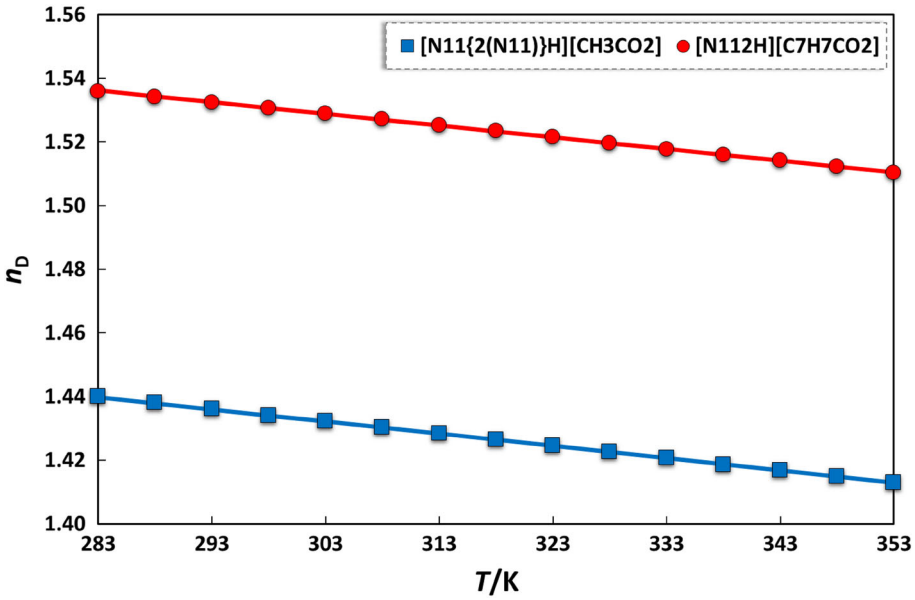

Fig. 3 Refractive index data for the studied PILs. The *solid lines* represent the Gardas and Coutinho group contribution method [54]

Table 5 Group contribution parameters, a_{i,n_D} and b_{i,n_D}, determined using the Gardas and Coutinho group contribution method for the refractive index [54]

Ionic Species	a_{i,n_D}	$10^4 \cdot b_{i,n_D}/K^{-1}$
Cation		
$[N_{11\{2(N11)\}H}]^+$	1.4101	3.28
$[N_{112H}]^+$ [36]	1.3792	2.78
Anion		
$[CH_3CO_2]^-$ [36]	0.1387	0.566
$[C_7H_7CO_2]^-$	0.2611	0.902

The derived molar refractions (R_m), free volumes (f_m), and polarizabilities were additionally determined as follows [55–57]:

$$\frac{\alpha_0}{4\pi\varepsilon_0} = \left(\frac{n_D^2 - 1}{n_D^2 + 2}\right)\frac{3M}{4\pi\rho N_A} \tag{6}$$

$$R_m = \frac{N_A\alpha_0}{3\varepsilon_0} = \frac{n_D^2 - 1}{n_D^2 + 2} \times V_m \tag{7}$$

$$f_m = V_m - R_m \tag{8}$$

where α_0 the electronic polarizability, ε_0 the vacuum permittivity, ρ the compound density, M the molecular weight and N_A the Avogadro number. The obtained values for these properties are reported in Table 3. As for the molar volume, density and refractive index,

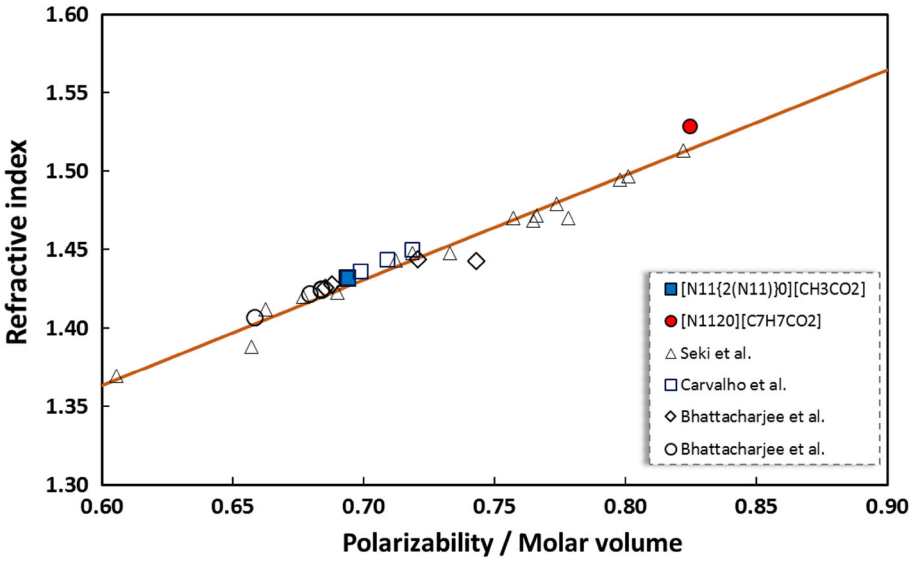

Fig. 4 Relationship between the refractive index and polarizability/molar volume for the two PILs at 303.15 K. The *unfilled triangles* and the *solid line* represent the experimental data and the correlation of Seki et al. [58]. The *unfilled squares*, *diamonds* and *circles* represent the experimental data reported in previous works [45, 46, 59]

$[N_{112H}][C_7H_7CO_2]$ also presents higher free volumes, molar refractions and polarizabilities than $[N_{11\{2(N11)\}H}][CH_3CO_2]$.

Recently, based on the premise that refractive indices are an indication of the dielectric response to an electrical field, induced by electromagnetic waves, and that refractive indices can be considered as the first order approximation response to electronic polarization within an instantaneous time scale, Seki et al. [58] evaluated the refractive indices of 17 ILs, as a function of temperature, against theoretical polarizabilities obtained through ab initio calculations and proposed a correlation between the refractive index and the polarizability normalized in terms of the molecular volume. Following the work of Seki et al. [58] the correlation was extended [45, 46, 59] to ammonium-, sulfonium-, phosphonium-, piperidinium-, and pyridinium-based ILs and now to the ILs studied here, showing that this type of correlation stands as a simpler approach to determine the refractive index from polarizability and vice versa, within the uncertainty of the correlation, as shown in Fig. 4.

3.4 Surface Tension

The experimental surface tension data were determined at atmospheric pressure in the temperature range of 293–343 K for $[N_{112H}][C_7H_7CO_2]$ and 293–323 K for $[N_{11\{2(N11)\}H}][CH_3CO_2]$, as presented in Table 6 and Fig. 5. As discussed above, the volatility of $[N_{11\{2(N11)\}H}][CH_3CO_2]$ makes the surface tension determination, above 323 K, highly unstable, making the methodology and equipment used not adequate to accurately determine the compound's surface tension. The $[N_{112H}][C_7H_7CO_2]$ presents higher surface tensions than $[N_{11\{2(N11)\}H}][CH_3CO_2]$, indicating that despite the important role displayed by the cation through the air–liquid interface structural organization [60, 61], the anion nature and their impact on the IL structure and surface organization also present relevant roles. The higher intermolecular interactions of the phenylacetate anion together with the smaller $[N_{112H}]^+$ cation leads to a more organized arrangement and higher surface energy when compared with $[N_{11\{2(N11)\}H}][CH_3CO_2]$.

The surface thermodynamic properties, namely, the surface entropy and the surface enthalpy, were derived using the quasi linear dependence (with an uncertainty of ± 0.1 $mN{\cdot}m^{-1}$) of the surface tension with temperature.

The surface entropy (S^{γ}), can be calculated according to the following equation [62, 63],

Table 6 Surface tension (γ), for the studied ILs as function of temperature and at atmospheric pressure

$[N_{11\{2(N11)\}H}][CH_3CO_2]$		$[N_{112H}][C_7H_7CO_2]$	
T/K	γ/mN·m^{-1}	T/K	γ/mN·m^{-1}
293.3	33.6	293.2	43.6
298.3	33.3	303.2	42.7
303.2	32.6	313.1	41.6
313.2	31.6	323.1	40.5
323.3	30.4	332.9	39.4
		343.0	38.2

U_c is $U_c(\gamma) = 0.1$ mN·m^{-1}, with an expanded uncertainty at 95 % confidence level

Standard temperature uncertainty is $u(T) = \pm 0.1$ K and the combined expanded uncertainty

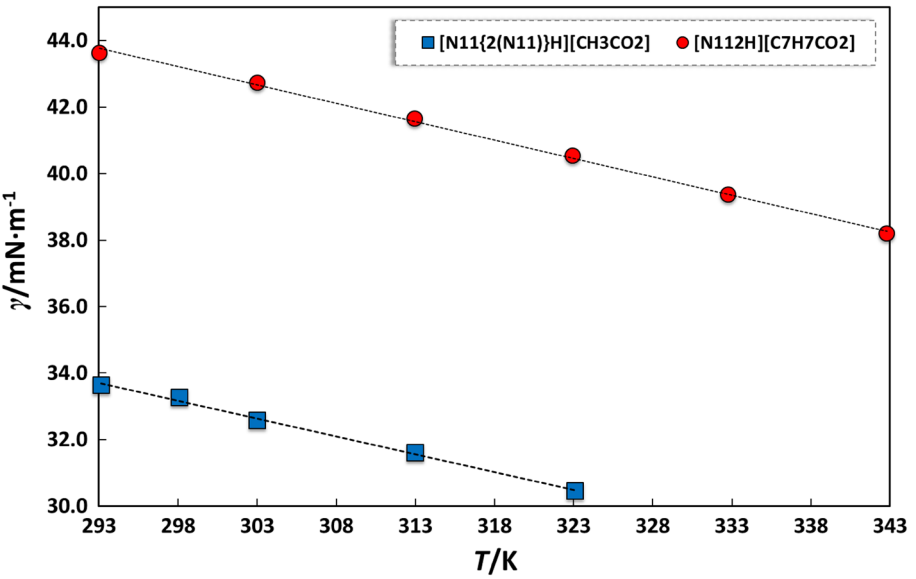

Fig. 5 Surface tension data for the studied PILs as a function of temperature. The *dotted lines* represent the linear fits to the experimental data

$$S^{\gamma} = -\left(\frac{\mathrm{d}\gamma}{\mathrm{d}T}\right) \tag{9}$$

while the surface enthalpy, H^{γ}, according to [62, 63],

$$H^{\gamma} = \gamma - T\left(\frac{\mathrm{d}\gamma}{\mathrm{d}T}\right) \tag{10}$$

where γ stands for the surface tension and T for the temperature.

The values of the thermodynamic functions for all of the ILs studied and the respective expanded uncertainties, derived from the slope of the curve $\gamma = f(T)$ in combination with the law of propagation of uncertainties, are presented in Table 3 [64].

The PILs display higher surface entropies than the aprotic ILs, suggesting a less structured liquid phase, in agreement with less prevalent hydrogen bonding due to their ionicity and proton transfer ability [36, 65].

The critical temperature of fluids is a significant thermophysical value regularly used in corresponding state correlations involving equilibrium and transport properties [66]. However, the direct determination of the critical temperatures of ILs is not feasible owing to the intrinsic nature of PILs together with negligible vapor pressures and relatively low decomposition temperatures. Rebelo et al. [67] proposed the use of the Eötvös [68] and Guggenheim [69] equations to estimate the hypothetical critical temperature of ILs, as described below,

$$\gamma\left(\frac{M}{\rho}\right)^{2/3} = K_{\mathrm{Eot}}(T_c - T) \tag{11}$$

$$\gamma = K_{\mathrm{Gug}}\left(1 - \frac{T}{T_c}\right)^{11/9} \tag{12}$$

where T_c is the critical temperature, M the molecular weight, ρ the density, K_{Eot} and K_{Gug} are fitted parameters. T_c, K_{Eot} and K_{Gug} were determined by fitting Eqs. 11 and 12 with the experimental data. Both equations are based on the fact that the surface tension becomes null at the critical point and although an overestimation of the critical temperature is expected, since at the critical point the pressure becomes the critical pressure, these equations provide reasonable estimations [66, 70]. The critical temperature values estimated from the surface tension data are summarized in Table 3. In agreement with the results obtained for other PILs studied in our previous work [36], the compounds here reported also present significantly lower critical temperatures than the AILs [45, 46, 60, 61].

4 Conclusions

Data for the density, viscosity, refractive index and surface tension of two ammonium-based PILs, $[N_{11\{2(N11)\}H}][CH_3CO_2]$ and $[N_{112H}][C_7H_7CO_2]$, were measured in the temperature range between 283.15 and 353.15 K and at atmospheric pressure and are here reported for the first time. Group contribution methods proposed by Gardas and Coutinho and the VFT equation were used to fit the refractive index and viscosity of the investigated ILs. The effects of the anion's aromaticity and of the cation's aliphatic tail size on the studied properties were discussed. The presence of an aromatic ring contributes to a more organized and compact bulk distribution, resulting from higher intermolecular interactions, thus exhibiting high density for $[N_{112H}][C_7H_7CO_2]$. This factor also leads to higher resistance to shear stress and therefore, higher viscosities of $[N_{112H}][C_7H_7CO_2]$ compared to $[N_{11\{2(N11)\}H}][CH_3CO_2]$. The higher intermolecular interactions of the phenylacetate anion together with the smaller $[N_{112H}]^+$ cation leads to a more organized arrangement and higher surface energy, compared with $[N_{11\{2(N11)\}H}][CH_3CO_2]$, thus presenting higher surface tensions for the former.

Acknowledgments This work was developed in the scope of the project CICECO-Aveiro Institute of Materials (Ref. FCT UID /CTM /50011/2013), financed by national funds through the FCT/MEC and when applicable co-financed by FEDER under the PT2020 Partnership Agreement. P.J.C. and A.B. also acknowledge FCT for their post-doctoral grants SFRH/BPD/82264/2011 and SFRH/BPD/77858/2011, respectively. M. G. Freire acknowledges the European Research Council (ERC) for the Starting Grant ERC-2013-StG-337753.

References

1. Wasserscheid, P., Welton, T.: Ionic Liquids in Synthesis. Wiley-VCH, Weinheim (2008)
2. Welton, T.: Room-temperature ionic liquids. Solvents for synthesis and catalysis. Chem. Rev. **99**, 2071–2084 (1999)
3. Wasserscheid, P., Keim, W.: Ionic liquids-new "solutions" for transition metal catalysis. Angew. Chem. Int. Ed. Engl. **39**, 3772–3789 (2000)
4. Hagiwara, R., Lee, J.: Ionic liquids for electrochemical devices. Electrochemistry **75**, 23–34 (2007)
5. Xiang, H.F., Yin, B., Wang, H., Lin, H.W., Ge, X.W., Xie, S., Chen, C.H.: Improving electrochemical properties of room temperature ionic liquid (RTIL) based electrolyte for Li-ion batteries. Electrochim. Acta **55**, 5204–5209 (2010)

6. Chowdhury, S., Mohan, R.S., Scott, J.L.: Reactivity of ionic liquids. Tetrahedron **63**, 2363–2389 (2007)
7. Sheldon, R.A., Lau, R.M., Sorgedrager, M.J., van Rantwijk, F., Seddon, K.R.: Biocatalysis in ionic liquids. Green Chem. **4**, 147–151 (2002)
8. Van Rantwijk, F., Sheldon, R.A.: Biocatalysis in ionic liquids. Chem. Rev. **107**, 2757–2785 (2007)
9. De Souza, R.F., Padilha, J.C., Gonçalves, R.S., Dupont, J.: Room temperature dialkylimidazolium ionic liquid-based fuel cells. Electrochem. Commun. **5**, 728–731 (2003)
10. Wang, Y., Zaghib, K., Guerfi, A., Bazito, F.F.C., Torresi, R.M., Dahn, J.R.: Accelerating rate calorimetry studies of the reactions between ionic liquids and charged lithium ion battery electrode materials. Electrochim. Acta **52**, 6346–6352 (2007)
11. Shvedene, N.V., Chernyshov, D.V., Pletnev, I.V.: Ionic liquids in electrochemical sensors. Russ. J. Gen. Chem. **78**, 2507–2520 (2009)
12. Wang, P., Zakeeruddin, S.M., Moser, J.E., Grätzel, M.: A new ionic liquid electrolyte enhances the conversion efficiency of dye-sensitized solar cells. J. Phys. Chem. B. **107**, 13280–13285 (2003)
13. Kennedy, D.F., Drummond, C.J.: Large aggregated ions found in some protic ionic liquids. J. Phys. Chem. B. **113**, 5690–5693 (2009)
14. Greaves, T.L., Drummond, C.J.: Protic ionic liquids: properties and applications. Chem. Rev. **108**, 206–237 (2008)
15. Bicak, N.: A new ionic liquid: 2-hydroxy ethylammonium formate. J. Mol. Liq. **116**, 15–18 (2005)
16. Iglesias, M., Torres, A., Gonzalez-Olmos, R., Salvatierra, D.: Effect of temperature on mixing thermodynamics of a new ionic liquid: {2-hydroxy ethylammonium formate (2-HEAF) + short hydroxylic solvents}. J. Chem. Thermodyn. **40**, 119–133 (2008)
17. Álvarez, V.H., Dosil, N., Gonzalez-Cabaleiro, R., Mattedi, S., Martin-Pastor, M., Iglesias, M., Navaza, J.M.: Brønsted ionic liquids for sustainable processes: synthesis and physical properties. J. Chem. Eng. Data **55**, 625–632 (2010)
18. Cota, I., Gonzalez-Olmos, R., Iglesias, M., Medina, F.: New short aliphatic chain ionic liquids: synthesis, physical properties, and catalytic activity in aldol condensations. J. Phys. Chem. B. **111**, 12468–12477 (2007)
19. Peric, B., Sierra, J., Martí, E., Cruañas, R., Garau, M.A., Arning, J., Bottin-Weber, U., Stolte, S.: (Eco)toxicity and biodegradability of selected protic and aprotic ionic liquids. J. Hazard. Mater. **261**, 99–105 (2013)
20. Pernak, J., Goc, I., Mirska, I.: Anti-microbial activities of protic ionic liquids with lactate anion. Green Chem. **6**, 323–329 (2004)
21. Hangarge, R.V., Jarikote, D.V., Shingare, M.S.: Knoevenagel condensation reactions in an ionic liquid. Green Chem. **4**, 266–268 (2002)
22. Laali, K.K., Gettwert, V.J.: Electrophilic nitration of aromatics in ionic liquid solvents. J. Org. Chem. **66**, 35–40 (2001)
23. Hu, Y., Chen, J., Le, Z., Zheng, Q.: Organic reactions in ionic liquids: ionic liquids ethylammonium nitrate promoted knoevenagel condensation of aromatic aldehydes with active methylene compounds. Synth. Commun. **35**, 739–744 (2005)
24. Poole, C.F.: Chromatographic and spectroscopic methods for the determination of solvent properties of room temperature ionic liquids. J. Chromatogr. A. **1037**, 49–82 (2004)
25. Susan, M.A.B.H., Noda, A., Mitsushima, S., Watanabe, M.: Brønsted acid-base ionic liquids and their use as new materials for anhydrous proton conductors. Chem. Commun. **8**, 938–939 (2003)
26. Earle, M., Plechkova, N., Seddon, K.: Green synthesis of biodiesel using ionic liquids. Pure Appl. Chem. **81**, 2045–2057 (2009)
27. Gálvez-Ruiz, J.C., Holl, G., Karaghiosoff, K., Klapötke, T.M., Löhnwitz, K., Mayer, P., Nöth, H., Polborn, K., Rohbogner, C.J., Suter, M., Weigand, J.J.: Derivatives of 1,5-diamino-1H-tetrazole: a new family of energetic heterocyclic-based salts. Inorg. Chem. **44**, 4237–4253 (2005)
28. Picquet, M., Tkatchenko, I., Tommasi, I., Wasserscheid, P., Zimmermann, J.: Ionic liquids, 3. Synthesis and utilisation of protic imidazolium salts in homogeneous catalysis. Adv. Synth. Catal. **345**, 959–962 (2003)
29. Talavera-Prieto, N.M.C., Ferreira, A.G.M., Simões, P.N., Carvalho, P.J., Mattedi, S., Coutinho, J.A.P.: Thermophysical characterization of N-methyl-2-hydroxyethylammonium carboxilate ionic liquids. J. Chem. Thermodyn. **68**, 221–234 (2014)
30. Greaves, T.L., Weerawardena, A., Fong, C., Drummond, C.J.: Many protic ionic liquids mediate hydrocarbon–solvent interactions and promote amphiphile self-assembly. Langmuir **23**, 402–404 (2007)
31. Belieres, J.-P., Angell, C.A.: Protic ionic liquids: preparation, characterization, and proton free energy level representation. J. Phys. Chem. B. **111**, 4926–4937 (2007)
32. Kurnia, K.A., Wilfred, C.D., Murugesan, T.: Thermophysical properties of hydroxyl ammonium ionic liquids. J. Chem. Thermodyn. **41**, 517–521 (2009)

33. Iglesias, M., Gonzalez-Olmos, R., Cota, I., Medina, F.: Brønsted ionic liquids: study of physicochemical properties and catalytic activity in aldol condensations. Chem. Eng. J. **162**, 802–808 (2010)
34. Pinkert, A., Ang, K.L., Marsh, K.N., Pang, S.: Density, viscosity and electrical conductivity of protic alkanolammonium ionic liquids. Phys. Chem. Chem. Phys. **13**, 5136–5143 (2011)
35. Chhotaray, P.K., Gardas, R.L.: Thermophysical properties of ammonium and hydroxylammonium protic ionic liquids. J. Chem. Thermodyn. **72**, 117–124 (2014)
36. Almeida, H.F.D., Passos, H., Lopes-da-Silva, J.A., Fernandes, A.M., Freire, M.G., Coutinho, J.A.P.: Thermophysical properties of five acetate-based ionic liquids. J. Chem. Eng. Data. **57**, 3005–3013 (2012)
37. Capelo, S.B., Méndez-Morales, T., Carrete, J., López Lago, E., Vila, J., Cabeza, O., Rodríguez, J.R., Turmine, M., Varela, L.M.: Effect of temperature and cationic chain length on the physical properties of ammonium nitrate-based protic ionic liquids. J. Phys. Chem. B. **116**, 11302–11312 (2012)
38. Chang-Ping, L., Zhuo, L., Ben-Xue, Z., Qing-Shan, L., Xiao-Xia, L.: Density, viscosity and conductivity of protic ionic liquid N,N-dimethylethanolammoniumpropionate. Acta Phys. Chim. Sin. **29**, 2157–2161 (2013)
39. Arfan, A., Bazureau, J.P.: Efficient combination of recyclable task specific ionic liquid and microwave dielectric heating for the synthesis of lipophilic esters. Org. Process Res. Dev. **9**, 743–748 (2005)
40. Govinda, V., Madhusudhana Reddy, P., Bahadur, I., Attri, P., Venkatesu, P., Venkateswarlu, P.: Effect of anion variation on the thermophysical properties of triethylammonium based protic ionic liquids with polar solvent. Thermochim. Acta **556**, 75–88 (2013)
41. Kavitha, T., Attri, P., Venkatesu, P., Devi, R.S.R., Hofman, T.: Influence of alkyl chain length and temperature on thermophysical properties of ammonium-based ionic liquids with molecular solvent. J. Phys. Chem. B. **116**, 4561–4574 (2012)
42. Carvalho, P.J., Regueira, T., Santos, L.M.N.B.F., Fernandez, J., Coutinho, J.A.P.: Effect of water on the viscosities and densities of 1-butyl-3-methylimidazolium dicyanamide and 1-butyl-3-methylimidazolium tricyanomethane at atmospheric pressure. J. Chem. Eng. Data **55**, 645–652 (2010)
43. Neves, C.M.S.S., Batista, M.L.S., Cláudio, A.F.M., Santos, L.M.N.B.F., Marrucho, I.M., Freire, M.G., Coutinho, J.A.P.: Thermophysical properties and water saturation of $[PF_6]$-based Ionic Liquids. J. Chem. Eng. Data **55**, 5065–5073 (2010)
44. Neves, C.M.S.S., Kurnia, K.A., Coutinho, J.A.P., Marrucho, I.M., Lopes, J.N.C., Freire, M.G., Rebelo, L.P.N.: Systematic study of the thermophysical properties of imidazolium-based ionic liquids with cyano-functionalized anions. J. Phys. Chem. B. **117**, 10271–10283 (2013)
45. Bhattacharjee, A., Carvalho, P.J., Coutinho, J.A.P.: The effect of the cation aromaticity upon the thermophysical properties of piperidinium- and pyridinium-based ionic liquids. Fluid Phase Equilib. **375**, 80–88 (2014)
46. Bhattacharjee, A., Luís, A., Santos, J.H., Lopes-da-Silva, J.A., Freire, M.G., Carvalho, P.J., Coutinho, J.A.P.: Thermophysical properties of sulfonium- and ammonium-based ionic liquids. Fluid Phase Equilib. **381**, 36–45 (2014)
47. Almeida, H.F.D., Teles, A.R.R., Lopes-da-Silva, J.A., Freire, M.G., Coutinho, J.A.P.: Influence of the anion on the surface tension of 1-ethyl-3-methylimidazolium-based ionic liquids. J. Chem. Thermodyn. **54**, 49–54 (2012)
48. Gardas, R.L., Freire, M.G., Carvalho, P.J., Marrucho, I.M., Fonseca, I.M.A., Ferreira, A.G.M., Coutinho, J.A.P.: $P\rho T$ measurements of imidazolium-based ionic liquids. J. Chem. Eng. Data **52**, 1881–1888 (2007)
49. Blesic, M., Swadzba-Kwasny, M., Belhocine, T., Gunaratne, H.Q.N., Lopes, J.N.C., Gomes, M.F.C., Padua, A.A.H., Seddon, K.R., Rebelo, L.P.N.: 1-Alkyl-3-methylimidazolium alkanesulfonate ionic liquids, $[C_nH_{2n}^{+1}\text{mim}]$ $[C_kH_{2k}^{+1}SO_3]$: synthesis and physicochemical properties. Phys. Chem. Chem. Phys. **11**, 8939–8948 (2009)
50. Machanová, K., Boisset, A., Sedláková, Z., Anouti, M., Bendová, M., Jacquemin, J.: Thermophysical properties of ammonium-based bis{(trifluoromethyl)sulfonyl}imide ionic liquids: volumetric and transport properties. J. Chem. Eng. Data **57**, 2227–2235 (2012)
51. Kilaru, P., Baker, G.A., Scovazzo, P.: Density and surface tension measurements of imidazolium-, quaternary phosphonium-, and ammonium-based room-temperature ionic liquids: data and correlations. J. Chem. Eng. Data **52**, 2306–2314 (2007)
52. Turbomole, version 6.1; University of Karlsruhe and Forschungszentrum Karlsruhe GmbH: Karlsruhe, Germany. http://www.turbomole.com (2009). (Accessed 23 March 2015)
53. Eckert, A.K.F.: COSMOtherm Version C2.1 Release 01.08, COSMOlogic GmbH & Co. KG, Leverkusen, Germany (2006)
54. Gardas, R.L., Coutinho, J.A.P.: Group contribution methods for the prediction of thermophysical and transport properties of ionic liquids. AIChE J. **55**, 1274–1290 (2009)

55. Israelachvili, J.N.: Intermolecular and Surface Forces. Academic Press, San Diego (2011)
56. Goodwin, A.R.H., Marsh, K.N., Wakeham, W.A.: Measurement of the Thermodynamic Properties of Single Phases, IUPAC Experimental Thermodynamics, vol. VI. Elsevier, Amsterdam (2003)
57. Brocos, P., Pineiro, A., Bravo, R., Amigo, A.: Refractive indices, molar volumes and molar refractions of binary liquid mixtures: concepts and correlations. Phys. Chem. Chem. Phys. **5**, 550–557 (2003)
58. Seki, S., Tsuzuki, S., Hayamizu, K., Umebayashi, Y., Serizawa, N., Takei, K., Miyashiro, H.: Comprehensive refractive index property for room-temperature ionic liquids. J. Chem. Eng. Data **57**, 2211–2216 (2012)
59. Carvalho, P.J., Ventura, S.P.M., Batista, M.L.S., Schröder, B., Gonçalves, F., Esperança, J., Mutelet, F., Coutinho, J.A.P.: Understanding the impact of the central atom on the ionic liquid behavior: phosphonium vs ammonium cations. J. Chem. Phys. **140**, 064505 (2014)
60. Carvalho, P.J., Freire, M.G., Marrucho, I.M., Queimada, A.J., Coutinho, J.A.P.: Surface tensions for the 1-alkyl-3-methylimidazolium bis(trifluoromethylsulfonyl)imide ionic liquids. J. Chem. Eng. Data **53**, 1346–1350 (2008)
61. Freire, M.G., Carvalho, P.J., Fernandes, A.M., Marrucho, I.M., Queimada, A.J., Coutinho, J.A.P.: Surface tensions of imidazolium based ionic liquids: anion, cation, temperature and water effect. J. Colloid Interface Sci. **314**, 621–630 (2007)
62. Adamson, A.W., Gast, A.P.: Physical Chemistry of Surfaces. John Wiley, New York (1997)
63. McNaught, A.D., Wikinson, A.: Compendium of Chemical Therminology, IUPAC Recommendations. Blackwell Science, Cambridge (1997)
64. Miller, J.C., Miller, J.N.: Statistics for Analytical Chemistry. PTR Prentice Hall, Chichester (1993)
65. MacFarlane, D.R., Pringle, J.M., Johansson, K.M., Forsyth, S.A., Forsyth, M.: Lewis base ionic liquids. Chem. Commun. **18** 1905–1917 (2006)
66. Poling, B.E., Prausnitz, J.M., O'Connell, J.P.: The Properties of Gases and Liquids. McGraw-Hill, New York (2001)
67. Rebelo, L.P.N., Canongia Lopes, J.N., Esperança, J.M.S.S., Filipe, E.: On the critical temperature, normal boiling point, and vapor pressure of ionic liquids. J. Phys. Chem. B. **109**, 6040–6043 (2005)
68. Shereshefsky, J.L.: Surface tension of saturated vapors and the equation of Eötvös. J. Phys. Chem. **35**, 1712–1720 (1930)
69. Guggenheim, E.A.: The principle of corresponding states. J. Chem. Phys. **13**, 253–261 (1945)
70. Birdi, K.S. (ed.): Handbook of Surface and Colloid Chemistry. CRC Press, Boca Raton (1997)